

## A 3D MODEL TO ANALYSE THE BEHAVIOUR OF COMPOSITE LAMINATES SUBJECTED TO OUT-OF-PLANE LOADINGS

Alfonso L.\*<sup>1</sup>, Uguen A.<sup>1</sup>, Badulescu C.<sup>1</sup>, Cellard C.<sup>2</sup>, Sohier L.<sup>1</sup>, Carrere N.<sup>1</sup>

<sup>1</sup>Laboratoire brestois de mécanique et des systèmes, ENSTA Bretagne/Université de Brest/ENIB/UEB, ENSTA Bretagne, 2 rue François Verny, 29806 Brest Cedex 09, France

<sup>2</sup>Laboratoire brestois de mécanique et des systèmes, ENSTA Bretagne/Université de Brest/ENIB/UEB, UBO-IUP Génie Mécanique, 6 Avenue Victor Le Gorgeu, 29238 BREST Cedex 3, France

\* Corresponding Author: [alfonshu@ensta-bretagne.fr](mailto:alfonshu@ensta-bretagne.fr)

**Keywords:** Composite laminate, Failure, Strength analysis, Multiscale, Out-of-plane.

### Abstract

*This paper describes a 3D failure model identified through Arcan tests, to analyse the behaviour of a laminate composite subject to out-of-plane loadings. The proposed criterion is based on the Hashin's hypothesis and the interactions between tensile and shear out-of-plane loadings are taken into account. The out-of-plane stresses generated in the composite subjected to an Arcan test are studied in order to determine the stack sequence influence. Finally, the out-of-plane failure envelope is identified by experimental results. Different stacks orientations of a carbon/epoxy composite has been tested.*

### 1. Introduction

In the last few years, the use of composite laminates and their assemblies has drastically increased in almost all engineering applications, e.g. automotive, aerospace, medical prosthetics and sport devices. In these applications complex 3D loadings are often generated. Thus, the analysis of the behaviour of composite laminates under out-of-plane loadings is necessary to insure the design requirements. However, few experimental devices and failure models proposed in the literature take into account this aspect.

A modified Arcan test has been developed in previous studies in order to analyse the behaviour of adhesives, composite plates and bonded metal/composite assemblies subjected to out-of-plane tensile/shear loadings [1]. It has already been shown that this method allow us to obtain reliable results [2]. However, the identification of the strength needs a 3D finite element analysis that at this time it has not been performed. The aim of the present papers is to determinate thanks to an inverse identification, the out-of-plane envelope of a composite laminate.

First, a description of the modified Arcan specimen, the properties of the study materials and the composite failure criterion are presented. A particular attention is paid to the definition of the

local axes at the different scales. Then, the finite element model is presented and the numerical hypotheses are explained. Finally, the predictions of the failure criterion and the experimental results are successfully compared.

## 2. Modified Arcan test modelling

### 2.1. Geometry of the used modified Arcan device

The specimen geometry and the fixture system of the Arcan device have a very important influence into the stress distribution and leads to stress singularities in adhesive and composite plate. Consequently, both the specimen geometry and the set fixation have been defined by numerical FE-models in order to reduce this particularity [3]. The current specimen geometry used in this study, allows to avoid the stress concentration and obtain reliable results (Figure 1).

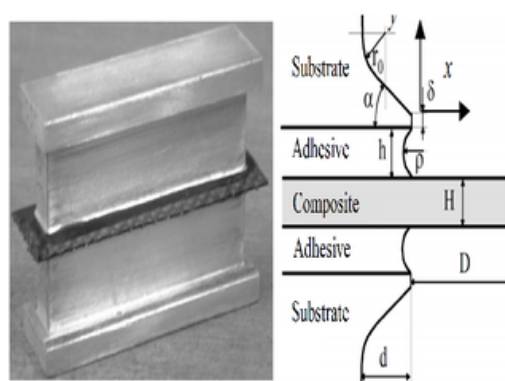


Figure 1. Modified Arcan specimen.

### 2.2. Materials

The simulations assume an elastic behavior of all materials. The substrates are made of aluminum and typical isotropic parameters are used (Young modulus  $E_{al} = 75GPa$ , Poissons ratio  $\nu_{al} = 0.3$ ). An epoxy Huntsman<sup>TM</sup>Araldite<sup>®</sup> 420 A/B adhesive is used to join the aluminium and the composite; its behaviour is also supposed isotropic ( $E_{ad} = 2GPa$ ,  $\nu_{ad} = 0.3$ ).

A carbon-epoxy laminate composite is used with different stack orientations (8 plies in the composite thickness). All plies are supposed with transverse isotropy and their parameters behaviours are shown in the Table 1.

Composite	Stack sequence	Unidirectional parameters			Thickness ply (mm)
		Young modulus (GPa)	Poisson 's ratio	Shear modulus (GPa)	
A1	8 UD (0°)				
A2	[+10° + 10° - 10° - 10°]s	$E_1 = 315$	$\nu_{12} = 0.3$	$G_{12} = 4.5$	
A3	[+20° + 20° - 20° - 20°]s	$E_2 = 6.75$	$\nu_{13} = 0.3$	$G_{13} = 4.5$	0.13
A4	[+30° + 30° - 30° - 30°]s	$E_3 = 6.75$	$\nu_{23} = 0.4$	$G_{23} = 4.5$	
A5	8 (+90°)				

Table 1. Properties of the composite laminates tested.

The Hashin's hypotheses [4] is assumed in order to distinguish three failure modes in the UD ply: the fiber mode, the in-plane interfiber mode and the out-of-plane interfiber mode (Figure 2). In the present study, a failure criterion based on [5] is used and only out-of-plane tensile failure is taken into account (Equation 1).

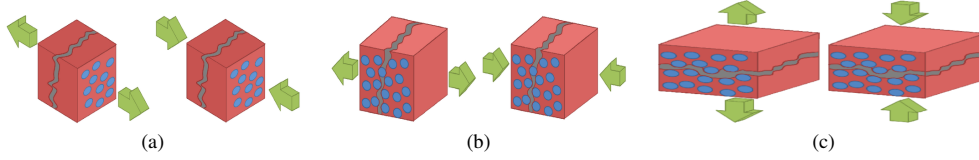


**Figure 2.** Tension and compression failure modes under Hashins hypotheses: fiber mode (a), in-plane inter-fiber mode (b) and out-of-plane inter-fiber mode (c).

$$f_{33}^2 = \left( \frac{\sigma_{33}}{Z_t} \right)^2 + \left( \frac{\tau_{13}}{S_{13}^R (1 - p_{13}\sigma_{33})} \right)^2 + \left( \frac{\tau_{23}}{S_{23}^R (1 - p_{23}\sigma_{33})} \right)^2 = 1 \quad (1)$$

Where  $Z_t$ ,  $S_{13}^R$  and  $S_{23}^R$  are respectively the out-of-plane tensile and shear strengths of a unidirectional ply. These parameters could be identified using an inverse identification procedure (see Section 4.2).

Under in-plane loadings, it has been shown that a transverse compression stress ( $\sigma_{22}^-$ ) increases the load transfer capability of the fiber/matrix and reduces the micro-damages due to shear loadings ( $\tau_{12}$ ). On the contrary, a transverse tensile stress ( $\sigma_{22}^+$ ) furthers the micro-damages and reduces the interfiber strengths of the composite [6]. Here, a similar hypothesis is made to take into account the interactions between out-of-plane tensile stress and out-of-plane shear stresses; it is represented by the  $(1 - p_{13}\sigma_{33})$  and  $(1 - p_{23}\sigma_{33})$  terms in Equation 1.

A previous in-plane study has identified the parameter  $p_{12}$  as a function of the transverse compressive strength  $Y_c$  ( $p_{12} = \frac{1}{Y_c}$ ) [5]. The out-of-plane parameters  $p_{13}$  and  $p_{23}$  obtained, for instance, with the modified Arcan test, needs multiaxial out-of-plane loadings.

### 2.3. Modelling of an Arcan test

The Arcan device used in this study allows loading a bonded assembly in mixed tensile/shear stresses using a simple tensile testing machine. There are three different scales in the test: the machine scale where a tensile loading is applied in the coordinate system  $UV$  (Figure 3a), the specimen scale where the out-of-plane tensile/shear state is created in the coordinate system  $X'Z'$  (Figure 3b) and the ply scale where the tensile stress ( $\sigma_{33}$ ) and the shear stresses ( $\tau_{13}$ ,  $\tau_{23}$ ) are defined in the coordinate system  $XZ$  (Figure 3c).

The angle of the loading ( $\gamma$ ) allows creating a tensile/shear state in the specimen (Figure 3b). In fact, when  $\gamma = 0^\circ$ , the bonded assembly is under out-of-plane tensile stress, when  $\gamma = 90^\circ$ , it is under out-of-plane shear stress; finally a mixed tensile/shear loading is presented when  $0^\circ < \gamma < 90^\circ$ . Naturally, it could be possible to have compression/shear loadings when  $90^\circ < \gamma < 180^\circ$ , but in this study only tensile/shear loads are assumed.

A second angle defines the orientation of the plies in the composite laminate ( $\theta$ ) (Figure 3c). This angle transfers the specimen loads (tensile/shear in  $X'Z'$  plane) into the coordinate system of each ply (Tensile/shear in XYZ space). In fact, a ply with  $\theta = 0^\circ$  will be loaded in the XZ plane ( $\sigma_{33}, \tau_{13}$ ), whereas a ply with  $\theta = 90^\circ$  will be loaded in the YZ plane ( $\sigma_{33}, \tau_{23}$ ).

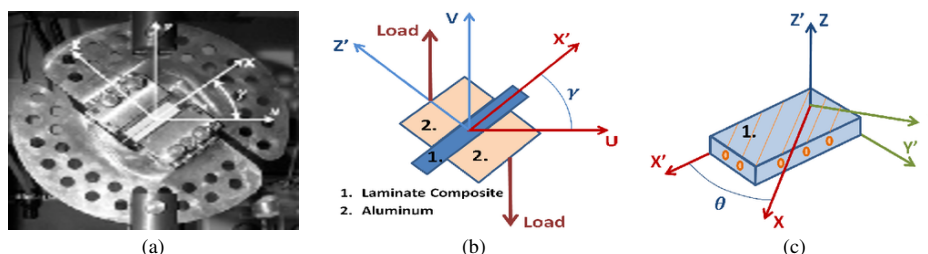


**Figure 3.** Coordinate systems in an Arcan device. Machine coordinate system (a), specimen coordinate system (b) and ply coordinate system (c).

#### 2.4. Types of loads

The Figure 4 shows the out-of-plane stress state for a ply with a  $\theta$  orientation and subjected to a  $\gamma$  loading orientation. An appropriate configuration of these angles enables us to subject the composite UD plies under four different stress states:

1.  $\sigma_{33}\tau_{13}$  stress state with  $\tau_{23}=0$ , this loading is created when  $\theta = 0^\circ$  and  $0^\circ < \gamma < 90^\circ$ . In practice, it is possible using the A1 stack orientation defined in Table 1 (See Figure 5a).
2.  $\sigma_{33}\tau_{23}$  stress state with  $\tau_{13}=0$ , this loading is created when  $\theta = 90^\circ$  and  $0^\circ < \gamma < 90^\circ$ . An A5 stack sequence is used in this case (See Figure 5b).
3.  $\tau_{13}\tau_{23}$  stress state with  $\tau_{33}=0$ , this loadings is created when  $\gamma = 90^\circ$  and  $0^\circ < \theta < 90^\circ$ . The A2-A3-A4 stack sequences can be used to get this state stress (See Figure 5c).
4.  $\sigma_{33}\tau_{13}\tau_{23}$  stress state, this case is the whole 3D out-of-plane criterion and it is defined with  $0^\circ < \gamma < 90^\circ$  and  $0^\circ < \theta < 90^\circ$ . A2-A3-A4 stack sequences are used to generate this stress state (See Figure 5d).

### 3. FE Modeling

The Arcan specimen is modeled using symmetries and anti-symmetries boundary conditions. It allows us to reduce the computing time and the machine requirements. The Figure 6 shows the two different models used in the Abaqus simulations.

Due to the edge effects presented in the adhesive/composite interface, the analysis of the stress distribution requires a refined mesh in the most highly stressed zones. 5 elements for a thickness of 0.1 mm were used in order to insure accurate and high quality results. The element type used to model the specimen is an 8-node linear brick element with reduced integration and hourglass control. All the displacements and loads are applied at the top surface of the substrates so as to be accurate to the experimental tests.

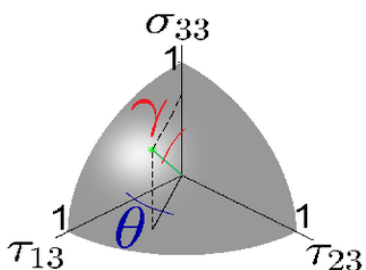


**Figure 4.** Angles  $\theta$  and  $\gamma$  in the 3D out-of-plane stress state.

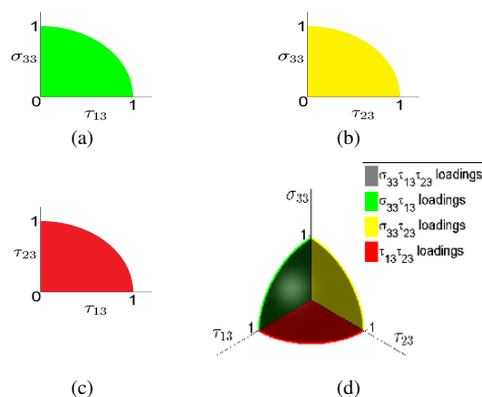


**Figure 5.** Types of loadings in an Arcan test.  $\tau_{13}\sigma_{33}$  loadings (a).  $\tau_{23}\sigma_{33}$  loadings (b).  $\tau_{13}\tau_{23}$  loadings (c) and  $\sigma_{33}\tau_{13}\tau_{23}$  loadings (d).

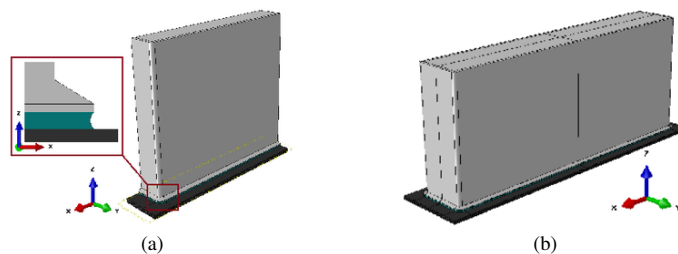


**Figure 6.** FE-Abaqus modeling with symmetry (a) and anti-symmetry (b) boundary conditions.

## 4. Results

### 4.1. Stress distribution

The five stack sequences have been tested under three different out-of-plane loadings: tensile ( $\gamma = 0^\circ$ ), tensile/shear ( $\gamma = 45^\circ$ ) and shear ( $\gamma = 90^\circ$ ). So as to provide a simple analysis of the results, only the maximal values of the stress state along the composite plate is considered. All stresses are also normalized to the maximal out-of-plane stress. The Figure 7 presents the evolution of the stress state for the three loadings with respect to the X' axis ( $x=x' \in [-25;25\text{mm}]$ , Figure 3-b).

Edge effects exist for all three loadings, however, it does not have any significant influence in relation to the critical stress. Thus, the critical zone is always placed in the center of each ply.

According to an intuitive prediction, when  $\gamma = 0^\circ$ , only the  $S_{33}$  stress has significant influence in the composite (Figure 7-a). Then, when  $\gamma = 45^\circ$  a mixed out-of-plane tensile/shear loading is created and the three out-of-plane stresses are important (Figure 7-b). Finally, when  $\gamma = 90^\circ$ , only the  $S_{13}$  and  $S_{23}$  stresses influence the composite behaviour (Figure 7-c).

### 4.2. Identification of the failure criterion

A particular aspect that attracts attention is that the stack sequence has very little influence under an out-of-plane tensile load. In fact, the finite element modeling shows that all the laminate

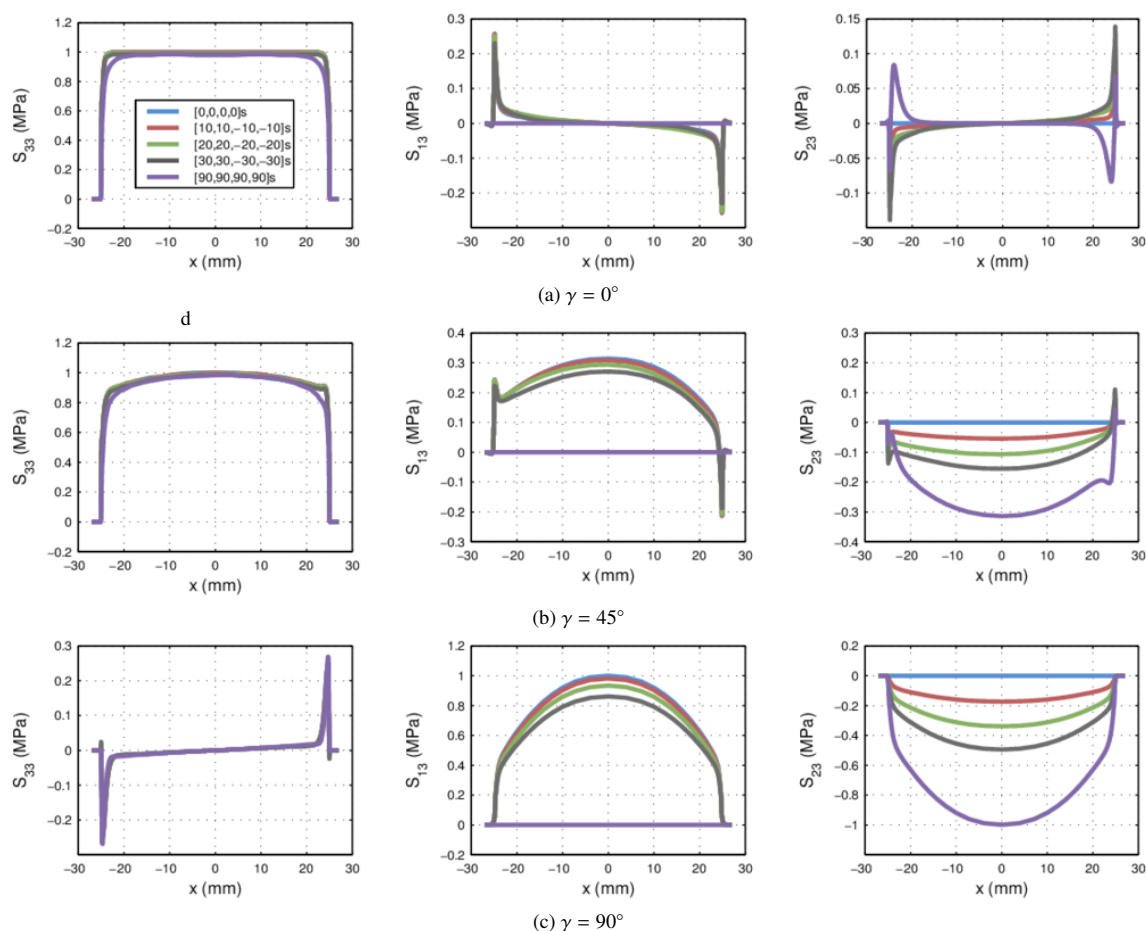


**Figure 7.** Normalized stress distribution in the composite under out-of-plane tensile loading (a), out-of-plane tensile/shear loading (b) and out-of-plane shear loading (c).

composites tested have the same  $S_{33}$  stress distribution and that the out-of-plane shear stresses could be negligible (Figure 7-a). It enables to identify the out-of-plane tensile strength  $Z_t$  by looking the numerical maximal out-of-plane  $S_{33}$  stress when the ultimate experimental tensile strength is applied.

The out-of-plane shear strength  $S_{13}^R$  is determined thanks to a UD composite plate (A1) subjected under a shear loading ( $\gamma = 90^\circ$ ). This configuration allows us to have an almost pure  $S_{13}$  stress in the composite (Figure 7-c). As in the previous case, the out-of-plane shear strength  $S_{13}^R$  value is determined by numerical simulations using the experimental ultimate shear strength.

To determinate the out-of-plane shear strength  $S_{23}^R$ , an A5 laminate plate (8[+90°]) is tested. In this case, an almost pure  $S_{23}$  stress is produced in the composite (Figure 7-c) and a similar methodology is used than that for determinate  $S_{13}^R$ .

### 4.3. Experimental results

Six specimens for each stack sequences have been tested under three different out-of-plane loadings (tensile,tensile/shear and shear). As shown in Figure 8, the failure is due to delamination

in the middle plane of the composite plate and the propagation is unstable.

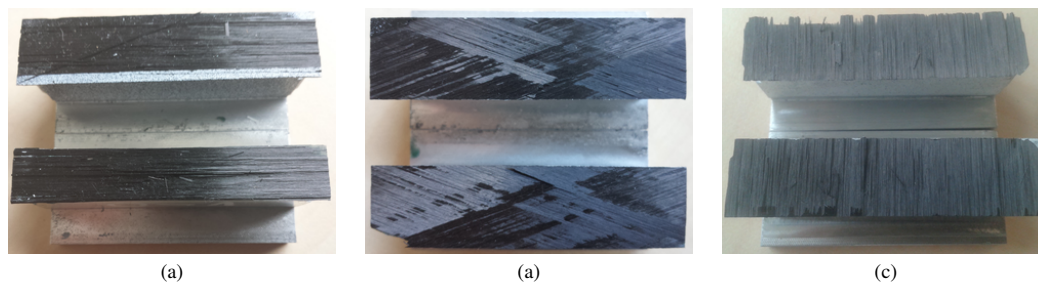


**Figure 8.** Typical composite plate failure for any out-of-plane loading. A1 stack sequence failure (a), A3 stack sequence failure (b) and A5 stack sequence failure(c).

As is shown Figure 9, a low scattering in the ultimate strength in the tensile test is observed for each stack orientation. It could be seen that a shear loading has a higher strength than a tensile shear.

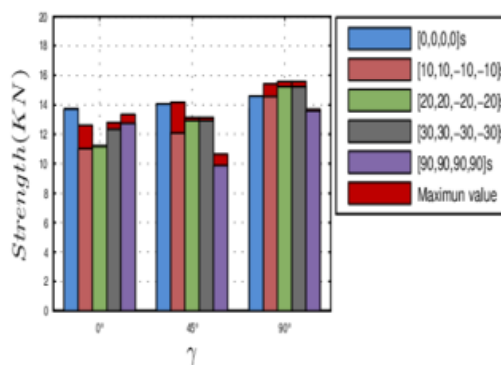


**Figure 9.** Minimum and maximum ultimate strength of a M55J/M18 laminate composite under different loadings and stack sequences. Results of an Arcan test.

The Figure 10 compares the predictions of the out-of-plane criterion previously identified and the experimental results. It can clearly be seen that the current criterion describes accurately the behaviour of the composite under out-of-plane tensile/shear loadings and for any stack sequence. In the same way, interactions between out-of-plane tensile/shear loadings are observed (Figure 10-a-b).

## 5. Conclusions

A 3D model approach has been proposed to analyse the behaviour of laminate plates subjected to a large tensile/shear out-of-plane loadings. The present approach is able to predict the stress state and the critical failure area of the laminate, which is essential in bonded assembly applications. At the same time, it has been shown that the fiber orientation, the stack sequence and the interactions between the out-of-plane loadings all have a very important influence on the out-of-plane strength of the laminate.

The stress state in the composite plate reflects the interaction of the out-of-plane tensile/shear loadings, in fact, in order to get an accurate 3D model, it is crucial to take into account the influence of the tensile loadings over the shear failure degradation.

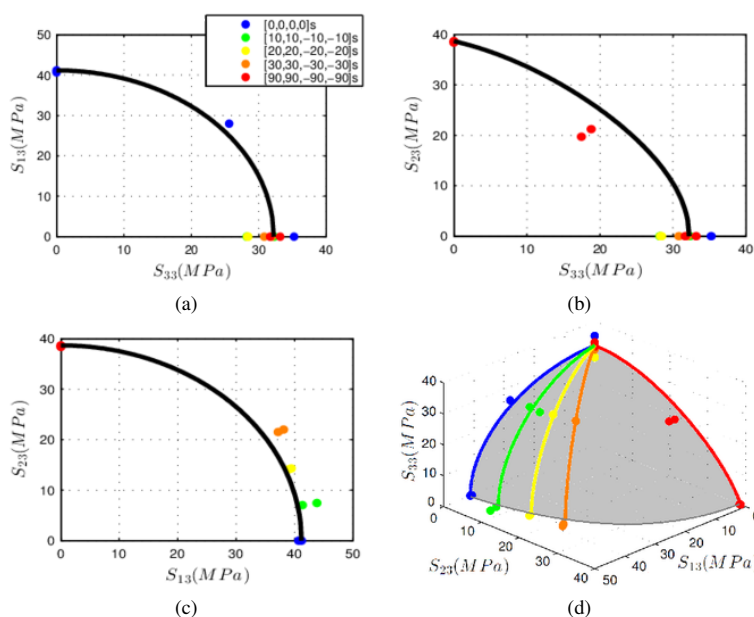


**Figure 10.** 3D Criterion predictions under different loadings.  $\sigma_{33}\tau_{13}$  loadings (a).  $\sigma_{33}\tau_{23}$  loadings (b).  $\sigma_{13}\tau_{23}$  loadings (c) and  $\sigma_{33}\tau_{13}\tau_{23}$  loadings (d).

A good agreement with experimental data results evidences that the current model estimates accurately the ultimate failure strength. Future work includes the consideration of plasticity in both composite and adhesive, and the analysis of ply thickness influence.

## References

- [1] Cognard JY, Davies P, Gineste B, and Sohier L. Development of an improved adhesive test method for composite assembly design. *Composites Science and Technology*, 65:359–368, 2005.
- [2] Cognard JY, Davies P, Sohier L, and Crac’hades R. A study of the non-linear behaviour of adhesively-bonded composite assemblies. *Composite Structures*, 76:34–36, 2006.
- [3] Cognard JY, Sohier L, and Davies P. A modified arcana test to analyze the behavior of composites and their assemblies under out-of-plane loadings. *Composites Part A: Applied science and manufacturing*, 42:111121, 2011.
- [4] Hashin Z. Failure criteria for unidirectional fiber composites. *Journal of Applied Mechanics*, 47:329–334, 1980.
- [5] Charrier JS. *Développement de méthodologies dédiées à l’analyse robuste de la tenue de structures composites sous chargements complexes tridimensionnels*. PhD thesis, École Nationale Supérieure d’Arts et Métiers, 2013.
- [6] Laurin F, Carrere N, and Maire J-F. A multiscale progressive failure approach for composite laminates based on thermodynamical viscoelastic and damage models. *Composites Part A: Applied science and manufacturing*, 38:198209, 2007.